

Regular two-component bouncing cosmologies and perturbations therein

V. Bozza^{a,b,c} and G. Veneziano^{d,e}

^a *Centro Studi e Ricerche “Enrico Fermi”, via Panisperna 89/A, Rome, Italy.*

^b *Dipartimento di Fisica “E. R. Caianiello”, Università di Salerno, I-84081 Baronissi, Italy.*

^c *Istituto Nazionale di Fisica Nucleare, Sezione di Napoli, Naples, Italy.*

^d *CERN, PH Dept., TH Unit, CH-1211 Geneva 23, Switzerland.*

^e *Collège de France, 11 place Marcelin Berthelot, F-75005 Paris, France.*

(Dated: November 6, 2018)

We present a full investigation of scalar perturbations in a rather generic model for a regular bouncing universe, where the bounce is triggered by an effective perfect fluid with negative energy density. Long before and after the bounce the universe is dominated by a source with positive energy density, which may be a perfect fluid, a scalar field, or any other source with an intrinsic isocurvature perturbation. Within this framework, we present an analytical method to accurately estimate the spectrum of large-scale scalar perturbations until their reentry, long after the bounce. We also propose a simple way to identify non-singular gauge-invariant variables through the bounce and present the results of extensive numerical tests in several possible realizations of the scenario. In no case do we find that the spectrum of the pre-bounce growing mode of the Bardeen potential can be transferred to a post-bounce constant mode.

I. INTRODUCTION

Motivations for studying bouncing cosmologies come from today’s widespread belief that a consistent theory of quantum gravity should cure the initial cosmological singularity –as well as other singularities that plague General Relativity (GR)– by a suitable modification of its short-distance behaviour. In the context of string theory, bouncing cosmologies of different kinds emerge as the most reasonable alternative to the Big Bang singularity. In the pre-bounce phase, as one goes to past-infinity, the universe is driven towards a non-singular attractor where generic initial conditions can be chosen.

The first proposal of a bouncing string cosmology was the so-called Pre-Big Bang scenario [1], which exploits the non-minimal coupling of the dilaton in superstring theory to drive a Pre-Big Bang super-inflationary epoch, ending when higher-order derivatives and/or loop corrections become non-negligible. A second realization of the same idea was given by the ekpyrotic/cyclic scenario [2], inspired by Horawa–Witten braneworlds [3]. Here the pre-bounce is characterized by the slow approach of two parallel branes, which eventually collide and then move away, giving rise to an ordinary expanding universe on each of the two branes. Both scenarios, when viewed in a four-dimensional Einstein frame, can be represented by a universe bouncing from contraction to a standard expansion.

A crucial test for any cosmological model lies on its capability of accounting for the origin, the growth and the spectrum of the fluctuations needed to explain the large-scale structures and the anisotropies in the cosmic microwave background. It is well known that observations require a nearly scale-invariant spectrum for the Bardeen potential. Such a spectrum can be naturally provided by the initial quantum fluctuations of the inflaton in the standard inflationary picture [4]. Alternatively, it can be provided by the initial isocurvature perturbations of an

other field, as in the “curvaton” mechanism [5], which is naturally implemented through the axion field in the Pre-Big Bang scenario [6]. A third possibility, the claim that the ekpyrotic scenario could directly provide (without appealing to the curvaton mechanism) a scale-invariant spectrum of adiabatic density perturbations, has given rise to a considerable debate about the correct way to describe the effects of a bounce on cosmological perturbations [7].

The main point at issue here concerns the Bardeen potential: it certainly grows very large, with a red or scale-invariant spectrum, during the pre-bounce phase. Does this mode survive the bounce or does it decay away, allowing other modes to take over? The use of classical matching conditions for perturbation through a space-like hypersurface [8] (which assume the continuity of the comoving curvature ζ) is not trivial in the case of a bounce, since the Hubble rate changes sign and the null energy condition (NEC) is necessarily violated for some time during the bounce. Then, more exotic matching conditions cannot be excluded, depending on the physics of the bounce [9].

In this situation, the only possibility to test some general arguments is to construct explicit models of regular bounces where the final spectrum of the Bardeen potential can be explicitly evaluated. In the context of GR, the more conservative possibility is to study closed universes, where the bounce is possible without violating the NEC [10]. In this case, the presence of the curvature scale is responsible for an explicit momentum dependence in the transfer matrix from pre- to post-bounce perturbations.

On the other hand, if one wants to stick to spatially flat cosmologies, a very good approximation presumably after a long pre-bounce epoch, one has to introduce a negative energy-density component that determines the transition from a contracting universe to an expanding one, dominated by a standard component, such as radiation. In this respect, Peter & Pinto-Neto [11] stud-

ied a bounce induced by a ghost scalar field, which connects a radiation-dominated contraction to a radiation-dominated expansion. Surprisingly they found that the Bardeen potential keeps the spectrum of its pre-bounce growing mode. Similar conclusions have been found by Finelli [12] in a model with two perfect fluids (one with negative energy density).

On the other hand, explicit bounce examples have been built using only one scalar field and triggering the bounce by higher derivatives and loop corrections to the Einstein equations [13] or by potentials involving integrals on spatially flat sections of a compact universe [14]. Both these one-component examples pointed at a complete post-bounce decay of the Bardeen pre-bounce growing mode.

Coming back to two-component models, Allen & Wands [15] found again a decay of the Bardeen pre-bounce growing mode in a cosmology dominated by a scalar field with a tracking potential (which allows it to mimic the background evolution of any kind of fluids), with the bounce triggered by a ghost scalar field. The reasons why the conclusions of this work are in contrast with those of Ref. [11] remained unclear.

In this paper we would like to bring more clarity in the investigation of regular bouncing cosmologies by introducing a rather generic cosmological model, which includes, as particular cases in a much wider parameter space, all previous models containing two non-interacting components. We find that the pre-bounce growing mode of the Bardeen potential always matches a decaying mode in the post-bounce, leaving no trace in the final spectrum at horizon re-entry. Our analysis proves that the claims in Refs. [11, 12] are incorrect, while it confirms the results of Ref. [15], generalizing to a much larger class of two-component bouncing cosmologies. A short summary of our results was anticipated in Ref. [16].

In this work we provide all the details of the analysis summarized in Ref. [16]. In particular, we explicitly provide the steps necessary to produce the analytical estimates from the method sketched in Ref. [16]. Moreover, we present the numerical studies of the cosmological perturbations in the whole parameter space, testing and supporting the analytical estimates. Finally, we expand the discussion on the gauge-choice issue and the way to construct non-singular gauge-invariant variables.

In Sect. 2, we introduce the class of backgrounds we want to consider, write down all the equations, and discuss the general behaviour of our background quantities. In Sect. 3, we introduce scalar perturbations, discuss the gauge issue, introduce the most convenient gauge-invariant quantities for our analysis, and discuss the vacuum normalization of perturbations that provides the initial conditions for our analysis. In Sect. 4, we describe the method used for analytical estimates and provide all the necessary steps for a systematic approach of the problem. In Sect. 5, we discuss these estimates throughout the parameter space that describes our bouncing cosmologies. In Sect. 6, we numerically check all the estimates discussed in Sect. 5. Finally, Sect. 7 contains a

discussion of the results.

II. A GENERAL MODEL FOR TWO-COMPONENT BOUNCING COSMOLOGIES

A common criticism against bouncing cosmologies triggered by a ghost scalar field –or negative energy matter– is that they deal with unphysical sources that are plagued by quantum instabilities and/or inconsistencies. However, we must keep in mind that the “true” bounce should be the outcome of a short-distance modification of GR, such as those coming from String/M-theory. Once we choose to perform an effective description in the Einstein frame, we cannot avoid (in a spatially flat cosmology) violations of the NEC in the sense that the short-distance corrections must enter as an effective negative energy (or pressure) contributions to the right-hand side of Friedman’s equations. Unless this is accepted, one must give up using the tools of GR and wait for the full String/M-theory to tell us how scalar perturbations behave during the high-energy phase.

In this paper we assume that a General Relativity description is indeed possible (at least for modes that are far outside the horizon during the bounce) and that the high-energy corrections can be modelled as an effective new negative-energy density field ρ_b , which becomes negligible as soon as we go far from the bounce itself. At this point it makes no sense to worry about the quantum instabilities of such an effective field, since the quantum description of high-energy corrections can only be done in the full mother theory. Nevertheless, nothing prevents the investigation of classical perturbations with the standard tools of GR.

The class of models we investigate in this paper have the following characteristics:

- The universe is filled by two components a and b , with energy density $\rho_a > 0$ and $\rho_b < 0$, respectively.
- Far from the bounce, ρ_a dominates the evolution of the universe, while ρ_b is important only at the bounce and becomes subdominant elsewhere.
- The two components do not decay and interact only gravitationally.
- Far from the bounce, the ratios

$$\Gamma_m = p'_m/\rho'_m, \quad m = a, b, \quad (1)$$

are asymptotically constant, that is we have a stable attractor in the past (implying also $w_m = p_m/\rho_m = \Gamma_m$).

The Friedman equations for a two-component cosmology can be simply written as

$$3\mathcal{H}^2 = a^2\rho \quad (2)$$

$$\mathcal{H}^2 + 2\mathcal{H}' = -a^2p \quad (3)$$

$$\rho' + 3\mathcal{H}(\rho + p) = 0, \quad (4)$$

where a prime denotes the derivative w.r.t. conformal time η , a is the scale factor, $\mathcal{H} = a'/a$ is the conformal Hubble rate, and we are using units such that $8\pi G = 1$. The total energy density is the sum of the individual energy densities of the two cosmological components $\rho = \rho_a + \rho_b$, and the same happens for the pressure $p = p_a + p_b$. Since the two fluids have neither interactions nor decay, they satisfy the continuity equation (4) independently.

As a consequence of the constancy of Γ_m , the attractor in the past is described by the following power laws

$$a(\eta) \simeq |\eta|^q \quad (5)$$

$$\mathcal{H} \simeq \frac{q}{\eta} \quad (6)$$

$$\rho_a \simeq \frac{3q^2}{|\eta|^{2+2q}} \quad (7)$$

$$\rho_b \simeq -\frac{3q^2}{|\eta|^{3q(1+\Gamma_b)}} \quad (8)$$

$$q = \frac{2}{1+3\Gamma_a}. \quad (9)$$

Here we have already chosen a convenient normalization for the scale factor and for the conformal time η , so that the two fluids have comparable energy densities at $\eta \simeq -1$. Of course, the condition $\rho_b/\rho_a \rightarrow 0$ for $\eta \rightarrow -\infty$ is satisfied if and only if $\Gamma_b > \Gamma_a$.

The power-law solution holds until $\eta \sim -1$. Then the bounce occurs at $\eta = 0$, when \mathcal{H} changes sign and finally at some time $\eta \sim 1$ the post-bounce expanding power-law solution is established with the same Γ_a and Γ_b as in the pre-bounce, so that Eqs. (5)-(9) hold again. In practice, we allow the bounce to be asymmetric within the range $|\eta| \lesssim 1$, but require the asymptotic power laws to be the same before and after the bounce. Actually, this final assumption could be easily relaxed, but we do not know any explicit example of two-components regular bounce with different pre- and post-bounce power laws. In Fig. 1 we show typical behaviours of the background functions.

III. SCALAR PERTURBATIONS

The perturbed line element, including only scalar perturbations, is

$$ds^2 = a^2(\eta) \left\{ (1+2\phi)d\eta^2 - 2B_{,i}d\eta dx^i - [(1-2\psi)\delta_{ij} + 2E_{,ij}] dx^i dx^j \right\}, \quad (10)$$

while the perturbed energy-momentum tensor of each source reads:

$$(T_m)^\mu{}_\nu = \begin{pmatrix} \rho_m + \delta\rho_m & -(\rho_m + p_m)\mathcal{V}_{m,j} \\ (\rho_m + p_m)\mathcal{V}_{m,i} & -(p_m + \delta p_m)\delta_{ij} + \Xi_{m,ij} \end{pmatrix} \quad (11)$$

with $m = a, b$ respectively; \mathcal{V}_m is the velocity potential and Ξ_m is the anisotropic stress. It is worth recalling the effects of a gauge transformation on each of these

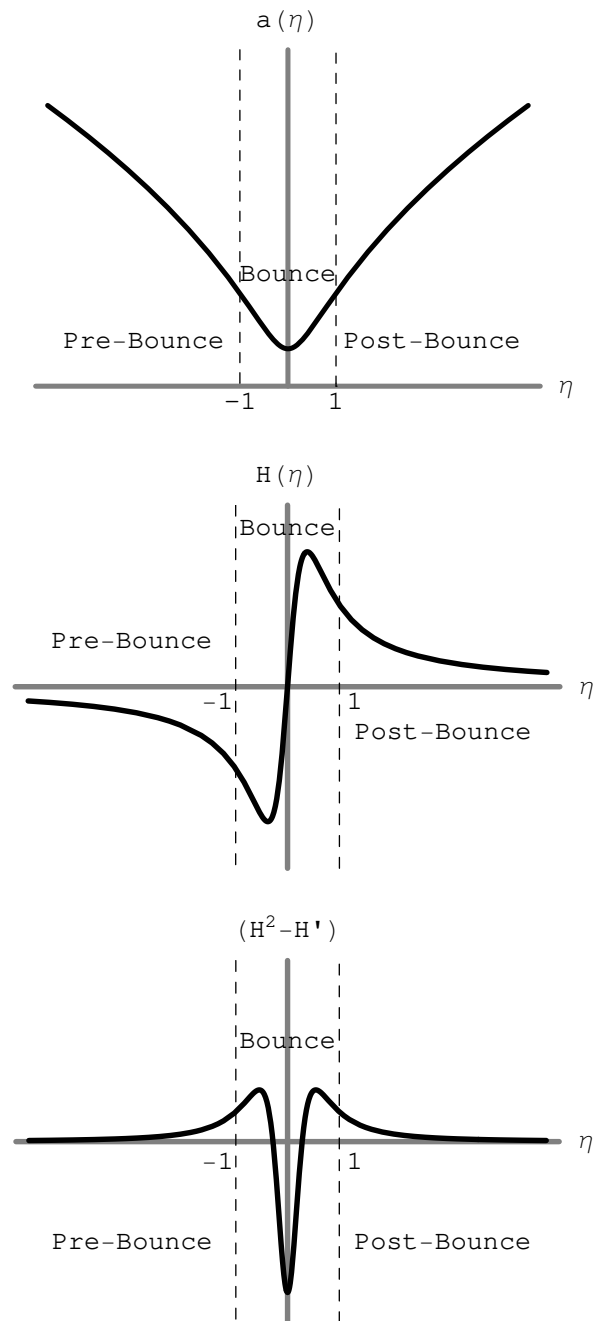


FIG. 1: Typical behaviours of the background functions in a bouncing cosmology. At the top we have the scale factor, in the middle the conformal Hubble parameter \mathcal{H} , and at the bottom the function $(\mathcal{H}^2 - \mathcal{H}') = a^2(\rho + p)/2$, which becomes negative when NEC violation occurs. The borders of the bounce phase have been put in evidence by vertical dashed lines at the times $\eta = \pm 1$.

variables. For an infinitesimal coordinate change

$$\eta \rightarrow \tilde{\eta} = \eta + \xi^0, \quad x^i \rightarrow \tilde{x}^i = x^i + \delta^{ij} \xi_{,j}, \quad (12)$$

the scalar perturbations are modified in the following way:

$$\tilde{\phi} = \phi - \mathcal{H}\xi^0 - \xi^{0'} \quad (13)$$

$$\tilde{\psi} = \psi + \mathcal{H}\xi^0 \quad (14)$$

$$\tilde{B} = B + \xi^0 - \xi' \quad (15)$$

$$\tilde{E} = E - \xi \quad (16)$$

$$\tilde{\delta\rho}_i = \delta\rho_i - \rho'_i \xi^0 \quad (17)$$

$$\tilde{\delta p}_i = \delta p_i - p'_i \xi^0 \quad (18)$$

$$\tilde{\mathcal{V}}_i = \mathcal{V}_i - \xi^0. \quad (19)$$

A. A general model for source perturbations

In order to close the system of equations, for each component we need to specify a relation between the perturbative variables. Since we want to make a single treatment for both perfect fluids and scalar fields, we need a general enough relation, containing both kinds of sources as particular cases. We therefore impose, for the dominant source,

$$\delta p_a = c_a^2 \delta \rho_a + \alpha (\rho_a + p_a) \mathcal{V}_a, \quad \alpha = \frac{p'_a - c_a^2 \rho'_a}{\rho_a + p_a}, \quad (20)$$

while for the secondary component we choose perfect fluid relations

$$\delta p_b = c_b^2 \delta \rho_b, \quad c_b^2 = \Gamma_b. \quad (21)$$

We also assume the anisotropic stress Ξ_m to vanish for both components.

In general, we allow Γ_a and c_a^2 to be different, opening the possibility of a non-vanishing α . In order to better understand the physical meaning of c_a^2 and α we can go to the comoving gauge with respect to the dominant fluid ($\mathcal{V}_a = 0$). We then have

$$c_a^2 = \frac{\delta p_a|_{\mathcal{V}_a=0}}{\delta \rho_a|_{\mathcal{V}_a=0}}, \quad (22)$$

which identifies c_a as the sound speed of the a -fluid. In fact, this quantity is properly defined in the frame where the fluid is at rest. We will see later that, indeed, c_a is the velocity of propagation of fluctuations in the a -fluid, thus explaining our somewhat unconventional notation.

The perfect fluid relation is recovered when the equality $\Gamma_a = c_a^2$ holds. In fact, in this case, we simply have $\alpha = 0$ and the pressure perturbation is just proportional to the density perturbation in any gauge with the same coefficient $\Gamma_a = c_a^2$. On the other hand, if $\Gamma_a \neq c_a^2$, we have $\alpha \neq 0$, implying the presence of an intrinsic isocurvature mode

$$\tau_a \delta S_a = \delta p_a - (p'_a / \rho'_a) \delta \rho_a = \alpha (\rho_a + p_a) (\mathcal{V}_a - \delta \rho_a / \rho'_a). \quad (23)$$

In particular, a scalar field φ with a self-interaction potential $V(\varphi)$ has

$$\rho_a = \frac{\varphi'^2}{2a^2} + V(\varphi), \quad p_a = \frac{\varphi'^2}{2a^2} - V(\varphi), \quad (24)$$

$$\delta \rho_a = \frac{\varphi'}{a^2} \delta \varphi' - \phi \frac{\varphi'^2}{a^2} + V'(\varphi) \delta \varphi, \quad \mathcal{V}_a = \frac{\delta \varphi}{\varphi'}, \quad (25)$$

$$\delta p_a = \frac{\varphi'}{a^2} \delta \varphi' - \phi \frac{\varphi'^2}{a^2} - V'(\varphi) \delta \varphi, \quad (26)$$

while the covariant conservation of the energy-momentum tensor gives

$$\varphi'' + 2\mathcal{H}\varphi' + a^2 V'(\varphi) = 0. \quad (27)$$

It is immediate to prove that Eq. (20) holds with $c_a^2 = 1$ and $\alpha = -2a^2 V_{,\varphi} / \varphi'$. Notice that a free scalar field is completely equivalent to a perfect fluid with stiff equation of state, $p = \rho$, while the presence of any potential inevitably introduces an intrinsic isocurvature mode.

From this discussion, we conclude that Eq. (20) is general enough to contain perfect fluids, scalar fields and any source with an intrinsic isocurvature mode generated according to Eq. (23). This ensures our treatment of a wide generality and, in particular, it allows us to include all previously studied models as particular cases.

B. The gauge issue

Sooner or later, all authors studying the problem of the evolution of cosmological perturbations through the bounce have met a non-trivial difficulty in making a convenient choice of the gauge. The commonly used longitudinal gauge makes the Bardeen potential appear directly as one entry of the perturbed metric. Typically, this variable becomes very large in the approach to the bounce, making the validity of the perturbative approach questionable. Other commonly used gauges introduce explicit divergences at the NEC violation or at the bounce. Under some circumstances, a safe gauge is provided by setting to zero the perturbation of a scalar field whose time derivative never changes sign [14, 15].

Our approach is to assume the existence of a regular gauge where all the components of the metric and of the energy-momentum tensors stay finite. In order for the linear theory to be valid, the perturbations should also stay small. If no regular gauge exists, then we have to conclude that the background is not a stable solution of Einstein equations and thus it is uninteresting as a cosmological model. Our approach will be applicable to all regular bounces that are stable solutions of the Einstein equations. In practical terms, a regular gauge must have ϕ , ψ , $B_{,i}$, $E_{,ij}$, $\delta \rho_m$, δp_m and $(\rho_m + p_m) \mathcal{V}_m$ finite and small ($m = a, b$). Notice that it is the combination $(\rho_m + p_m) \mathcal{V}_m$ that enters the energy-momentum tensor of the m -source. This means that \mathcal{V}_m can possibly diverge

when $(\rho_m + p_m)$ goes to zero provided the above product stays finite. The same happens for the total velocity potential:

$$\mathcal{V} = (\rho + p)^{-1} \sum_{m=a,b} (\rho_m + p_m) \mathcal{V}_m, \quad (28)$$

which may diverge at the NEC violation, the product $(\rho + p)\mathcal{V}$ staying finite.

Using the regular gauge, it is easy to construct gauge-invariant combinations that are regular and can thus be safely used to follow perturbations through the bounce. Indeed, the Bardeen potential

$$\Psi = \psi + \mathcal{H}(E' - B) \quad (29)$$

is a regular combination of regular perturbations. Old matching conditions suggest to use the comoving curvature perturbation $\zeta = \psi + \mathcal{H}\mathcal{V}$. However, the presence of the velocity potential does not protect this variable from possible divergences. We propose to use instead

$$\tilde{\zeta} = (\mathcal{H}^2 - \mathcal{H}')(\psi + \mathcal{H}\mathcal{V}), \quad (30)$$

which is guaranteed to be regular, since $2(\mathcal{H}^2 - \mathcal{H}')\mathcal{V} = a^2(\rho + p)\mathcal{V}$ is finite in the regular gauge. We then introduce individual gauge-invariant variables

$$\tilde{\zeta}_m = \frac{1}{2}a^2(\rho_m + p_m)(\psi + \mathcal{H}\mathcal{V}_m) \quad (31)$$

$$\Psi_m = \frac{1}{2}a^2(\rho'_m \psi + \mathcal{H}\delta\rho_m), \quad (32)$$

which are also regular by construction. Of course

$$\tilde{\zeta} = \tilde{\zeta}_a + \tilde{\zeta}_b. \quad (33)$$

Before proceeding with the perturbation equations, it is worth commenting briefly on the commonly used gauges. Using the transformations (13)–(19), we can pass from the (assumed) regular gauge to any other gauge. These transformations may either explicitly induce divergences, or ensure that the variables in the transformed gauge are regular as well. Let us analyse some cases explicitly.

The zero-curvature gauge ($\tilde{\psi} = 0$), obtained by the regular gauge setting $\xi = -\psi\mathcal{H}^{-1}$, introduces terms with \mathcal{H}^{-1} in ϕ , B and \mathcal{V}_i , which diverge at the bounce.

The comoving gauge ($\tilde{V} = 0$), obtained by setting $\xi^0 = \mathcal{V}$, introduces \mathcal{V} in all other variables. As said before, \mathcal{V} can diverge at the NEC violation.

The synchronous gauge ($\tilde{\phi} = \tilde{B} = 0$) is obtained by setting $\xi^0 = a^{-1} \int a\phi d\eta$ and $\xi = \int B d\eta + \int d\eta a^{-1} \int a\phi d\eta'$. This transformation induces no divergences and so we can say that if a regular gauge exists where all perturbations are finite, then the variables in the synchronous gauge are also finite.

Similarly, for the longitudinal gauge ($\tilde{E} = \tilde{B} = 0$), obtained by setting $\xi = E$ and $\xi^0 = B - E'$, no divergence is introduced.

The uniform density gauge ($\tilde{\delta\rho} = 0$) is obtained by setting $\xi^0 = \delta\rho/\rho'$. By the continuity equation, we see that the transformed variables have to diverge both at the NEC violation and at the bounce $\mathcal{H} = 0$.

Concerning a possible ‘‘uniform pressure gauge’’ ($\tilde{\delta p} = 0$, obtained by setting $\xi^0 = \delta p/p'$) it is difficult to say something general. However, it is hard to imagine a model where p' does not vanish at any time during the bounce.

The uniform individual density or pressure gauges have a similar fate. They typically introduce divergences at the bounce. The gauge comoving with one of the components, instead, introduces divergences only if \mathcal{V}_m itself diverges, but this is not necessarily true. The regularity of the gauges in Refs [13, 14, 15] can be understood in the light of this remark.

Among those just described, the synchronous and longitudinal gauges are the only ones that keep all the variables finite. Yet we know that in the longitudinal gauge $\psi = \Psi$ and the Bardeen potential grows very large in the approach to the bounce. Indeed, the finiteness of all variables does not assure their smallness. In this case, one can still consider the variables in the longitudinal gauge as useful auxiliary mathematical quantities: the transformation to longitudinal-gauge variables has to be regarded as a simple mathematical change of variables, without the physical meaning of a coordinate transformation. Nevertheless, nothing prevents one from solving the equations in the longitudinal-gauge variables and then discuss the results with gauge-invariant quantities, whose physical interpretation is clear. In fact, the longitudinal variables have the important property of being regular (even if large) and thus can be used to go through the bounce safely.

C. Perturbation equations

Let us start by perturbing the Einstein equations. The 00, $i0$, ii , $i \neq j$ components respectively read

$$a^2\delta\rho + 6\mathcal{H}(\mathcal{H}\phi + \psi') + 2k^2[\psi + \mathcal{H}(E' - B)] = 0 \quad (34)$$

$$2(\mathcal{H}\phi + \psi') = a^2(\rho + p)\mathcal{V} \quad (35)$$

$$-\frac{1}{2}a^2\delta p + \mathcal{H}^2\phi + 2\mathcal{H}'\phi + \mathcal{H}\phi' + 2\mathcal{H}\psi' + \psi'' = 0 \quad (36)$$

$$\psi - \phi + 2\mathcal{H}(E' - B) + (E'' - B') = 0. \quad (37)$$

We can use Eq. (35) to eliminate ϕ , Eqs. (20) and (21) for δp_m , Eqs. (31) and (32) to eliminate $\delta\rho_m$ and \mathcal{V}_m , and finally Eq. (29) for ψ . Equations 00, ii and $i \neq j$ become

$$(3\tilde{\zeta} + k^2\Psi)\mathcal{H} + \Psi_a + \Psi_b = 0 \quad (38)$$

$$\tilde{\zeta}' = (\alpha - \mathcal{H})\tilde{\zeta}_a - \mathcal{H}\tilde{\zeta}_b + c_a^2\Psi_a + c_b^2\Psi_b \quad (39)$$

$$\Psi' + \frac{2\mathcal{H} - \mathcal{H}'}{\mathcal{H}^2}\Psi = \frac{\tilde{\zeta}}{\mathcal{H}}, \quad (40)$$

where we have made use of the fact that $\tilde{\zeta}_a + \tilde{\zeta}_b = \tilde{\zeta}$.

The perturbations of the covariant conservation of the energy-momentum tensor of the first fluid, after using the Hamiltonian constraint (38), give

$$\begin{aligned} \tilde{\zeta}'_a + \frac{2\mathcal{H}(\mathcal{H} - \alpha) + a^2(\rho_b + p_b)}{2\mathcal{H}}\tilde{\zeta}_a - c_a^2\Psi_a &= \\ &= \frac{a^2(\rho_a + p_a)}{2\mathcal{H}}\tilde{\zeta}_b \end{aligned} \quad (41)$$

$$\begin{aligned} \Psi'_a + \frac{6c_a^2\mathcal{H}^2 + a^2(\rho + p + \rho_a + p_a)}{2\mathcal{H}}\Psi_a + a^2\frac{\rho_a + p_a}{2\mathcal{H}}\Psi_b \\ + \frac{2k^2 + 6\mathcal{H}\alpha + 3a^2(\rho_a + p_a)}{2}\tilde{\zeta}_a = -3a^2\frac{\rho_a + p_a}{2}\tilde{\zeta}_b. \end{aligned} \quad (42)$$

The perturbations of the covariant conservation of the energy-momentum tensor of the second fluid give the same equations with $a \leftrightarrow b$. The sum of Eq. (41) with its b counterpart yields Eq. (39), while the sum of Eq. (42) with its counterpart yields a linear combination of Eqs. (40) and (39).

Summing up, Eqs. (41) and (42) and their b counterparts are an independent set of coupled first-order differential equations, which completely describe cosmological perturbations in our problem in terms of the regular gauge-invariant variables $\tilde{\zeta}_a$, $\tilde{\zeta}_b$, Ψ_a and Ψ_b . The fact that \mathcal{H} appears in some denominators does not indicate that the differential equations break down at the bounce. Actually, one can easily check by the definitions (31) and (32) that the numerators also contain an \mathcal{H} factor multiplied by finite functions.

Later on, we shall widely use another set of variables to describe the system, namely $\tilde{\zeta}$, $\tilde{\zeta}_b$, Ψ and Ψ_b . This set has the advantage of including directly Ψ and $\tilde{\zeta}$, which are the most interesting quantities characterizing cosmological perturbations. In terms of these variables the set of differential equations becomes

$$\Psi' + \frac{2\mathcal{H}^2 - \mathcal{H}'}{\mathcal{H}}\Psi - \frac{\tilde{\zeta}}{\mathcal{H}} = 0 \quad (43)$$

$$\begin{aligned} \tilde{\zeta}' + (\mathcal{H} + 3c_a^2\mathcal{H} - \alpha)\tilde{\zeta} + c_a^2k^2\mathcal{H}\Psi = -\alpha\tilde{\zeta}_b \\ + (c_b^2 - c_a^2)\Psi_b \end{aligned} \quad (44)$$

$$\begin{aligned} \Psi'_b + \frac{\mathcal{H}^2(1 + 3c_b^2) - \mathcal{H}'}{\mathcal{H}}\Psi_b + k^2\tilde{\zeta}_b = \\ = \frac{a^2(\rho_b + p_b)}{2}k^2\Psi \end{aligned} \quad (45)$$

$$\tilde{\zeta}'_b + \frac{2\mathcal{H}^2 - \mathcal{H}'}{\mathcal{H}}\tilde{\zeta}_b - c_b^2\Psi_b = \frac{a^2(\rho_b + p_b)}{2\mathcal{H}}\tilde{\zeta}. \quad (46)$$

D. Vacuum normalization

Choosing initial conditions for the perturbations of the two components is by no means trivial. While for the dominant component we can choose ordinary vacuum normalization, for the secondary one this is quite an ar-

bitrary choice. In fact, we can think that the first component is an ordinary perfect fluid, a scalar field, or any other field initially in a vacuum state. On the contrary, on the basis of the former discussion about the nature of the secondary component, we cannot really justify giving a well-defined quantum initial state to this effective component. Yet, in order to compare our results with other works, which have systematically chosen the vacuum normalization even for the secondary component, we will follow this attitude as well. In the conclusions we will comment about the generality of our results and their (in)dependence on the initial state of the secondary-component perturbations.

Taking the derivatives of Eq. (41) and eliminating Ψ_a and Ψ'_a using Eqs. (41) and (42), we get a second-order equation for $\tilde{\zeta}_a$ coupled to $\tilde{\zeta}_b$ and Ψ_b . Of course, we also get an analogous second-order equation for $\tilde{\zeta}_b$. Introducing the Sasaki–Mukhanov canonical variables

$$v_m = \tilde{\zeta}_m/[c_m(\rho_m + p_m)^{1/2}\mathcal{H}], \quad (47)$$

the two equations can be written in a very compact way as

$$v''_a + (c_a^2k^2 - z''_a/z_a)v_a = O(\rho_b/\rho_a)^{1/2} \quad (48)$$

$$v''_b + (c_b^2k^2 - z''_b/z_b)v_b = O(\rho_b/\rho_a)^{1/2}, \quad (49)$$

with $z_a = a^2(\rho_a + p_a)^{1/2}/(c_a\mathcal{H})$ and $z_b = a^{(1+3c_b^2)}(\rho_b + p_b)^{1/2}/c_b$. Inside $O(\rho_b/\rho_a)^{1/2}$ we include all the terms where v_a , v_b appear multiplied by background functions going to zero asymptotically faster than $|\eta|^{-2}$ and terms where v'_a , v'_b are multiplied by functions going to zero faster than $|\eta|^{-1}$. All these terms become irrelevant in the asymptotic past and do not affect the initial vacuum normalization. We also see that c_m^2 multiplies the Laplacian of v_m and thus represents the velocity of propagation of the fluctuations in each component, confirming our statement in Sect. 2.

The asymptotic solutions of Eqs. (48) and (49) in the power law regime are

$$v_a = \sqrt{|\eta|}C_aH_{\nu_a}^{(1)}(c_ak|\eta|) \quad (50)$$

$$v_b = \sqrt{|\eta|}C_bH_{\nu_b}^{(1)}(c_bk|\eta|), \quad (51)$$

where $H_{\nu}^{(1)}$ is the Hankel function of the first kind, C_a and C_b are pure numbers of order 1, and

$$\nu_a = \frac{1}{2} - q \quad (52)$$

$$\nu_b = \frac{1}{2}(3c_b^2q - 1 - q). \quad (53)$$

Now that we have established the initial conditions for the Mukhanov variables, we can derive those for $\tilde{\zeta}_a$ and $\tilde{\zeta}_b$ from Eq. (47). For Ψ_a and Ψ_b we can use Eq. (41) and the corresponding equation for $\tilde{\zeta}'_b$.

IV. EVOLUTION OF PERTURBATIONS

In this section we shall estimate the behaviour of perturbations before and after the bounce, giving a complete discussion of the final momentum and time dependences in terms of the parameters of the cosmological model.

The first step is to rewrite Eqs. (43)–(46) in their integral form

$$\Psi = \frac{\mathcal{H}}{a^2} \left[\frac{c_1(k)}{k^2} + \int \frac{a^2}{\mathcal{H}^2} \tilde{\zeta} d\eta \right], \quad (54)$$

$$\begin{aligned} \tilde{\zeta} = a^2(\rho_a + p_a) & \left[c_2(k) - \int \frac{c_a^2 \mathcal{H}}{a^2(\rho_a + p_a)} k^2 \Psi d\eta \right. \\ & \left. - \int \frac{\alpha}{a^2(\rho_a + p_a)} \tilde{\zeta}_b d\eta + \int \frac{c_b^2 - c_a^2}{a^2(\rho_a + p_a)} \Psi_b d\eta \right], \quad (55) \end{aligned}$$

$$\begin{aligned} \Psi_b = \frac{\mathcal{H}}{a^{1+3c_b^2}} & \left[c_3(k) - \int \frac{a^{1+3c_b^2} k^2}{\mathcal{H}} \tilde{\zeta}_b d\eta \right. \\ & \left. + \int \frac{a^{3+3c_b^2}(\rho_b + p_b)}{2\mathcal{H}} k^2 \Psi d\eta \right], \quad (56) \end{aligned}$$

$$\begin{aligned} \tilde{\zeta}_b = a^{1+3c_b^2} \mathcal{H}(\rho_b + p_b) & \left[c_4(k) + \int \frac{c_b^2}{a^{1+3c_b^2} \mathcal{H}(\rho_b + p_b)} \Psi_b d\eta \right. \\ & \left. + \int \frac{a^{1-3c_b^2}}{2\mathcal{H}^2} \tilde{\zeta} d\eta \right]. \quad (57) \end{aligned}$$

In these equations, each variable is expressed as the sum of the solution of the associated homogeneous differential equation, carrying an arbitrary constant $c_i(k)$, plus several integrals of the other variables, representing the coupling terms. This structure is particularly useful to study perturbations outside the horizon as the ones we are interested in. Indeed we shall limit our attention to modes with $k \ll 1$, i.e. to modes which exit the horizon long before the bounce and reenter much later. For these modes, horizon-exit can still be described by the asymptotic decoupled solutions (50) and (51).

As a result, we can match the expansions (54)–(57) to the long-wavelength limit of the asymptotic solutions. As a practical example, let us examine $\tilde{\zeta}$, which far from the bounce is dominated by $\tilde{\zeta}_a$. Through Eq. (50) and (47), the vacuum normalization provides the following expression in the long-wavelength limit for this variable

$$\tilde{\zeta}_a \sim k^{-\nu_a} |\eta|^{-2} + k^{\nu_a} |\eta|^{-1-2q}, \quad (58)$$

where all the background functions have been replaced by their power-law behaviours (5)–(9).

Equation (55) in the power-law limit gives

$$\tilde{\zeta} \sim |\eta|^{-2} [c_2(k) + c_1(k)|\eta|^{1-2q} + c_0(k)], \quad (59)$$

where we have used Eq. (54) to evaluate the integral of Ψ and we have kept only the lowest-order terms in $k\eta$. The integration constant $c_0(k)$ can be simply absorbed in the definition of $c_2(k)$.

At this point, in order to match the two expressions (58) and (59), it is sufficient to impose

$$c_1(k) \sim k^{\nu_a}, \quad c_2(k) \sim k^{-\nu_a}, \quad (60)$$

where we have discarded any numerical factor of order 1, as we shall do throughout our analysis. In the same way, matching $\tilde{\zeta}_b$, we obtain

$$c_3(k) \sim k^{-\nu_b}, \quad c_4(k) \sim k^{\nu_b}. \quad (61)$$

Defining $\vec{F}(\eta) = (\Psi, \tilde{\zeta}, \Psi_b, \tilde{\zeta}_b)$, we can write the system (54)–(57) in the compact form

$$\vec{F}(\eta) = \vec{F}^{(0)}(\eta) + B(\eta) \int A(\eta) \vec{F}(\eta) d\eta, \quad (62)$$

where

$$\begin{aligned} \vec{F}^{(0)}(\eta) = & \left(\frac{\mathcal{H}}{a^2} \frac{c_1(k)}{k^2}, a^2(\rho_a + p_a) c_2(k), \right. \\ & \left. \frac{\mathcal{H}}{a^{1+3c_b^2}} c_3(k), a^{1+3c_b^2} \mathcal{H}(\rho_b + p_b) c_4(k) \right) \quad (63) \end{aligned}$$

is the vector of the homogeneous solutions, $B(\eta)$ and $A(\eta)$ are two matrices that can be easily read from Eqs. (54)–(57). All these quantities are just combinations of the background functions. Then we can construct the full solution of Eq. (62) recursively

$$\vec{F}(\eta) = \vec{F}^{(0)}(\eta) + \sum_{i=1}^{\infty} \vec{F}^{(i)}(\eta) \quad (64)$$

$$\vec{F}^{(i)}(\eta) = B(\eta) \int A(\eta) \vec{F}^{(i-1)}(\eta) d\eta. \quad (65)$$

The whole problem is thus reduced to the calculation of a sufficient number of terms in the sum (64), which are reduced to multiple integrals of background functions. In the following subsections we shall illustrate how to calculate these integrals in the pre-bounce, during the Bounce and after the Bounce.

A. Pre-bounce evolution

As long as the power-law behaviours (5)–(9) remain valid, the evaluation of all integrals can be easily done. In fact, a generic integrand $f(\eta)$ can be expanded as $c_i(k)|\eta|^s$ giving

$$\int_{\eta}^{\eta} c_i(k) |\eta|^s d\eta \sim c_i(k) |\eta|^{s+1}, \quad \eta < -1. \quad (66)$$

Calculating iteratively the integrals, we can safely stop at $\vec{F}^{(2)}(\eta)$ since the next terms would just give higher and higher powers of $k|\eta|$ multiplying already existing terms (recall that we are interested in the evolution of modes

outside the horizon). Keeping now the lowest order in $k\eta$ of each mode, we find

$$\Psi \sim k^{\nu_a - 2} |\eta|^{-1-2q} + k^{-\nu_a} + k^{-\nu_b} |\eta|^{2-q(1+3c_b^2)} + C_a k^{\nu_b} |\eta|^{1-2q} \quad (67)$$

$$\tilde{\zeta} \sim k^{\nu_a} |\eta|^{-1-2q} + k^{-\nu_a} |\eta|^{-2} + k^{-\nu_b} |\eta|^{-q(1+3c_b^2)} + C_a k^{\nu_b} |\eta|^{-1-2q} \quad (68)$$

$$\Psi_b \sim k^{\nu_a} |\eta|^{-3q(1+c_b^2)} + k^{-\nu_a+2} |\eta|^{1-q(1+3c_b^2)} + k^{-\nu_b} |\eta|^{-1-q(1+3c_b^2)} + k^{\nu_b+2} |\eta|^{2-2q} \quad (69)$$

$$\tilde{\zeta}_b \sim k^{\nu_a} |\eta|^{1-3q(1+c_b^2)} + k^{-\nu_a} |\eta|^{-q(1+3c_b^2)} + k^{-\nu_b} |\eta|^{-q(1+3c_b^2)} + k^{\nu_b} |\eta|^{-1-2q}. \quad (70)$$

In this expression and in the following subsections, we introduce the factors

$$C_a = \begin{cases} k^2 \eta^2 & \alpha = 0 \\ 1 & \alpha \neq 0 \end{cases} \quad (71)$$

$$X_a = \begin{cases} k^2 & \alpha = 0 \\ 1 & \alpha \neq 0 \end{cases} \quad (72)$$

in order to write a single expression for the solutions that holds both when $\alpha \neq 0$ and when $\alpha = 0$.

In Eq. (67), we explicitly see the presence of a growing mode in Ψ carrying a red spectrum that becomes scale-invariant in the limit of slow contraction $q \rightarrow 0$. These pre-bounce solutions are valid until the energy density of the secondary fluid becomes comparable with the dominant one. At that point the power-law solution breaks down and the bounce phase starts. As we have fixed this time to $\eta = -1$, by evaluating Eqs. (67)–(70) at $\eta \simeq -1$, we obtain the order of magnitude of the different modes at the onset of the bounce. Since the only scale left in this evaluation is k , we deduce that the mode with the reddest spectrum always dominates at the bounce. This does not mean that the same mode will also dominate in the post-bounce, since, as we shall see later, many of these modes decay after the bounce.

B. The Bounce

We are not very interested in the specific evolution of all variables during the bounce. It is just interesting to observe that all homogeneous solutions $\vec{F}^{(0)}(\eta)$ can be easily followed through the bounce as they are directly expressed by combinations of background functions.

One thing that may worry the reader is the fact that some integrals contain diverging functions of the background. Actually the \mathcal{H}^{-1} in the integrals of Ψ and $\tilde{\zeta}_b$ in Eq. (56) and in the integral of Ψ_b in Eq. (57) are immediately compensated by \mathcal{H} factors in Ψ , $\tilde{\zeta}_b$ and Ψ_b inside the integrals. The solution is a bit more subtle for the integrals of $\tilde{\zeta}$ in Eqs. (54) and (57). For example, the integral of $\tilde{\zeta}$ in Eq. (54) contains a \mathcal{H}^{-2} , which diverges as $|\eta|^{-2}$. The integral thus diverges as $|\eta|^{-1}$,

but this divergence is compensated by the \mathcal{H} factor outside the brackets. The result is that the limit of Ψ as $\eta \rightarrow 0^-$ is finite. The same happens for the integral of $\tilde{\zeta}$ in (57). Then Eqs. (54)–(57) confirm the regularity of all variables through the bounce.

As we shall see later, we are interested in the integrals covering the whole bounce phase

$$\int_{-1}^1 f(\eta) d\eta. \quad (73)$$

The k -dependence factors out of the integral, and we are also integrating out the η dependence. We deduce that, in the absence of other scales that can enter the result, this integral must return a value with the same order of magnitude of $f(-1)$, which has been evaluated for all functions in the previous subsection using the pre-bounce power-law limit.

For the two integrals that diverge at the bounce, we can replace the integral (73) by its principal value

$$\lim_{\epsilon \rightarrow 0} \left[\int_{-1}^{-\epsilon} f(\eta) d\eta + \int_{\epsilon}^1 f(\eta) d\eta \right]. \quad (74)$$

This expression is consistent with the continuity of the gauge-invariant variables. As the two divergences compensate, the dimensional argument can be safely applied as before.

C. Post-bounce evolution

In the post-bounce, the evaluation of the homogeneous solutions $\vec{F}^{(0)}(\eta)$ is elementary, since they are directly expressed in terms of the background functions. In particular, we may notice that the pre-bounce growing mode of Ψ with the red spectrum $c_1(k)k^{-2}$ comes from the homogeneous solution, which becomes a decaying mode in the post-bounce. This does not automatically mean that this mode becomes irrelevant in the post-bounce. We need to show that no growing mode develops the same spectrum and that there is always at least one mode that dominates on this decaying mode at horizon re-entry.

In order to evaluate the integrals in the post-bounce, we split their integration domain into three pieces, respectively covering the pre-bounce, the Bounce and the post-bounce phase

$$\int_{-1}^{\eta} f(\eta) d\eta = \int_{-1}^{-1} f(\eta) d\eta + \int_{-1}^1 f(\eta) d\eta + \int_1^{\eta} f(\eta) d\eta. \quad (75)$$

These integrals give

$$\int_{-1}^{-1} c_i(k) |\eta|^s d\eta \sim c_i(k), \quad \int_{-1}^1 f(\eta) d\eta \sim c_i(k),$$

$$\int_1^\eta c_i(k) |\eta|^s d\eta \sim c_i(k) [\eta^{s+1} - 1]. \quad (76)$$

In fact, the first integral is Eq. (66) evaluated at $\eta = -1$. The second integral is Eq. (73), which gives a result of the same order of magnitude of the pre-bounce contribution. The last integral involves background functions in the post-bounce and can be safely evaluated using the power-law limit (5)–(9) again. Summing up, each integral gives a constant contribution plus a growing or decaying one, depending on the value of s . If $s < -1$ the integral is dominated by the constant contribution, which comes from regions close to the bounce and from the bounce itself, while if $s > -1$ the integral is dominated by the growing contribution at late times, far from the bounce. Note that any constant contribution, once generated, sums to the original homogeneous mode and follows the same evolution.

D. Post-bounce solution in a simplified example

In the former subsections we have explained how to calculate each single integral once the integrand has been specified. To construct the full solution, we need to proceed step by step, evaluating the integrals recursively. To explain this procedure, it is better to start with a simplified system.

Let us consider the subsystem $\Psi, \tilde{\zeta}$, without couplings to the secondary component. The starting point for the construction of the full post-bounce solution is given by the homogeneous solutions. We thus set

$$\Psi^{(0)} = \frac{\mathcal{H}}{a^2} \frac{c_1(k)}{k^2} \sim c_1(k) k^{-2} \eta^{-1-2q} \quad (77)$$

$$\tilde{\zeta}^{(0)} = a^2 (\rho_a + p_a) c_2(k) \sim c_2(k) \eta^{-2}. \quad (78)$$

As said before, the homogeneous modes survive unchanged during the bounce and after the bounce.

The first step is to evaluate the integrals using the homogeneous modes

$$\Psi^{(1)} = \frac{\mathcal{H}}{a^2} \int \frac{a^2}{\mathcal{H}^2} \tilde{\zeta}^{(0)} d\eta \sim$$

$$c_2(k) \eta^{-1-2q} [\eta^{1+2q} - 1] \quad (79)$$

$$\tilde{\zeta}^{(1)} = -a^2 (\rho_a + p_a) \int \frac{c_a^2 \mathcal{H}}{a^2 (\rho_a + p_a)} k^2 \Psi^{(0)} d\eta \sim$$

$$c_1(k) \eta^{-2} [\eta^{1-2q} - 1]. \quad (80)$$

Every integral gives a time-dependent contribution and a constant one (taking also into account pre-bounce and Bounce contributions, which are of the same order).

As a second step, we calculate the integrals using $\Psi^{(1)}$ and $\tilde{\zeta}^{(1)}$

$$\Psi^{(2)} = \frac{\mathcal{H}}{a^2} \int \frac{a^2}{\mathcal{H}^2} \tilde{\zeta}^{(1)} d\eta \sim$$

$$c_1(k) \eta^{-1-2q} [\eta^2 - \eta^{1+2q} - 1] \quad (81)$$

$$\tilde{\zeta}^{(2)} = -a^2 (\rho_a + p_a) \int \frac{c_a^2 \mathcal{H}}{a^2 (\rho_a + p_a)} k^2 \Psi^{(1)} d\eta \sim$$

$$c_2(k) k^2 \eta^{-2} [\eta^2 - \eta^{1-2q} - 1]. \quad (82)$$

In the same way we can build $\Psi^{(3)}$ and $\tilde{\zeta}^{(3)}$, and so on. The complete solution is the sum of all the partial contributions

$$\Psi = \sum_{i=0}^{\infty} \Psi^{(i)} \quad (83)$$

$$\tilde{\zeta} = \sum_{i=0}^{\infty} \tilde{\zeta}^{(i)}. \quad (84)$$

However, since we are interested in the solution just before horizon re-entry, we can drop all terms that are just $k^2 \eta^2$ times some other term already present in the series. In fact, these terms determine the first oscillation of the mode at horizon re-entry. For example, the first term in the brackets of $\Psi^{(2)}$ and $\tilde{\zeta}^{(2)}$ are just $k^2 \eta^2$ times $\Psi^{(0)}$ and $\tilde{\zeta}^{(0)}$ respectively. The last terms in the same brackets are just k^2 times $\Psi^{(0)}$ and $\tilde{\zeta}^{(0)}$ respectively, so that they are just k^2 corrections to the homogeneous modes (remember that we are studying modes with $k \ll 1$). In this simplified example, all $\Psi^{(i)}$ and $\tilde{\zeta}^{(i)}$ with $i \geq 3$ give subleading terms according to this prescription. We are finally left with the following post-bounce solution

$$\Psi \sim k^{-\frac{3}{2}-q} \eta^{-1-2q} + k^{-\frac{1}{2}+q} +$$

$$k^{-\frac{1}{2}+q} \eta^{-1-2q} + k^{\frac{1}{2}-q} \quad (85)$$

$$\tilde{\zeta} \sim k^{-\frac{1}{2}+q} \eta^{-2} + k^{\frac{1}{2}-q} \eta^{-1-2q} +$$

$$k^{\frac{1}{2}-q} \eta^{-2} + k^{\frac{3}{2}+q} \eta^{-1-2q}, \quad (86)$$

where we have replaced $c_i(k)$ by their explicit spectral dependence.

For each variable, the first term is the homogeneous mode, the second and the third come from the integral of the homogeneous mode of the other variable, the fourth term is the only new term coming from the second recursion. Now we can discuss the evolution of these four modes in the post-bounce. We can distinguish two cases: fast contraction–expansion ($q > 1/2$) and slow contraction–expansion ($q < 1/2$).

Let us start by the case $q > 1/2$. Just after the bounce ($\eta \sim 1$), the dominant mode is always the reddest one. We see that Ψ is by far dominated by its homogeneous mode, while $\tilde{\zeta}$ is dominated by the integral of Ψ . However, when we evaluate the modes at horizon re-entry ($\eta \sim 1/k$), $\tilde{\zeta}$ is still dominated by the third mode, which comes from the integral of the homogeneous mode of Ψ

and in particular is the contribution coming from regions close to the bounce. On the contrary, at $\eta \sim 1/k$ the homogeneous mode of Ψ has decayed below the fourth mode in Eq. (85). This constant mode comes from the integral of the dominant mode of $\tilde{\zeta}$. This mode has the original spectrum of the homogeneous mode of Ψ multiplied by k^2 , which is typically blue.

In the case of slow evolution ($q < 1/2$), both Ψ and $\tilde{\zeta}$ are dominated by their homogeneous modes at the bounce ($\eta \sim 1$); $\tilde{\zeta}$ does not acquire a mode dominating its homogeneous mode and, consequently, the fourth mode of Ψ remains subdominant till re-entry. In this case, the dominant mode in Ψ at re-entry is still the homogeneous decaying mode, endowed with its red spectrum, which becomes scale-invariant in the limit $q \rightarrow 0$. Of course, this situation cannot be compatible with observations, since the potentially scale-invariant spectrum is carried by a decaying mode that becomes subdominant with respect to a constant mode just at horizon re-entry. Moreover, as we shall see later, the interplay with the secondary component (which we have neglected in this simplified treatment) is essential in this regime, since it provides those isocurvature modes that dominate at horizon re-entry.

The two cases of this simplified example are synthesized in Fig. 2, where we have plotted Ψ and ζ (which is more familiar than $\tilde{\zeta}$ to people working in cosmological perturbations). Following [15], we have chosen $\text{Log } a(\eta)$ as time coordinate. We see that in Fig. 2a, where we have chosen a model with $q > 1/2$, ζ grows in the pre-bounce, dominated by the integral of Ψ . Then it sets to a constant value in the post-bounce. The Bardeen potential growing mode turns into a decaying mode in the post-bounce, which becomes subdominant when Ψ becomes of the order of ζ . In Fig. 2b, where we have chosen a model with $q < 1/2$, $\zeta \simeq \eta^2 \tilde{\zeta}$ is dominated by its homogeneous (constant) mode in the pre-bounce and in the post-bounce. The decaying mode of Ψ becomes of the same order as the constant mode just at horizon re-entry. In this case, for very small q , we have an almost scale-invariant spectrum for the decaying mode of Ψ , while its constant mode has a blue spectrum.

Notice also the presence of two spikes in ζ before and after the bounce. These are the mentioned divergences at the NEC violation times, which make ζ unsuitable for the description of the evolution of scalar perturbations close to the bounce.

V. PERTURBATIONS AT THE ONSET OF HORIZON RE-ENTRY

In this section, we apply the method explained in the previous section to the whole system of integral equations governing our problem. We shall thus build the full solution of scalar perturbations in the post-bounce, keeping all the relevant modes. We shall then find out the dominant modes at the onset of horizon re-entry for

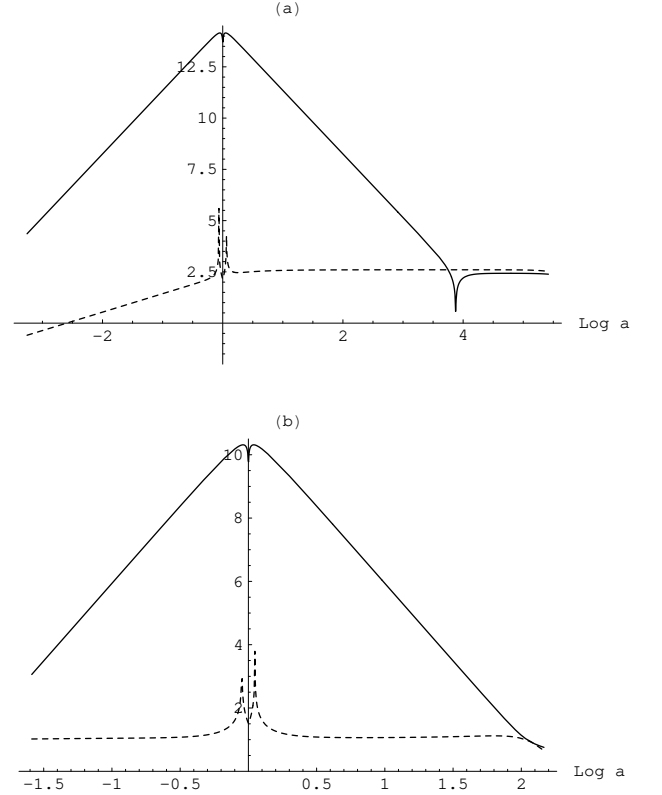


FIG. 2: (a) Simplified perturbations in a bouncing cosmology with $\alpha = 0$, $c_a^2 = 0.4$, $c_b^2 = 2.5$. The solid line is $\text{Log}|\Psi|$ and the dashed line is $\text{Log}|\zeta|$. (b) The same as (a) with $c_a^2 = 1.6$.

all gauge-invariant variables.

After four recursions in the integrations of Eqs. (54)–(57), no new modes are added to the post-bounce solution. Its final form reads

$$\begin{aligned} \Psi \sim & k^{\nu_a - 2} \eta^{-1 - 2q} + k^{\nu_a} + \\ & C_a k^{-\nu_a} \eta^{1 - 2q} + k^{-\nu_a} + \\ & C_a k^{-\nu_b} \eta^{1 - 2q} + X_a k^{-\nu_b} + \\ & C_a k^{\nu_b} \eta^{1 - 2q} + C_a k^{\nu_b}, \end{aligned} \quad (87)$$

$$\begin{aligned} \tilde{\zeta} \sim & k^{\nu_a} \eta^{-2} + k^{\nu_a} \eta^{-1 - 2q} + \\ & k^{-\nu_a} \eta^{-2} + C_a k^{-\nu_a} \eta^{-1 - 2q} + \\ & X_a k^{-\nu_b} \eta^{-2} + C_a k^{-\nu_b} \eta^{-1 - 2q} + \\ & C_a k^{\nu_b} \eta^{-2} + C_a k^{\nu_b} \eta^{-1 - 2q}, \end{aligned} \quad (88)$$

$$\begin{aligned} \Psi_b \sim & k^{\nu_a} \eta^{-1 - q(1 + 3c_b^2)} + X_a k^{\nu_a + 2} \eta^{-2q} + \\ & k^{-\nu_a + 2} \eta^{1 - q(1 + 3c_b^2)} + k^{-\nu_a + 2} \eta^{-2q} + \\ & k^{-\nu_b} \eta^{-1 - q(1 + 3c_b^2)} + k^{-\nu_b + 2} \eta^{-2q} + \\ & k^{\nu_b + 2} \eta^{1 - q(1 + 3c_b^2)} + k^{\nu_b + 2} \eta^{-2q}, \end{aligned} \quad (89)$$

$$\begin{aligned}
\tilde{\zeta}_b \sim & X_a k^{\nu_a} \eta^{-1-2q} + k^{\nu_a} \eta^{-q(1+3c_b^2)} + \\
& k^{-\nu_a} \eta^{-1-2q} + k^{-\nu_a} \eta^{-q(1+3c_b^2)} + \\
& k^{-\nu_b} \eta^{-1-2q} + k^{-\nu_b} \eta^{-q(1+3c_b^2)} + \\
& k^{\nu_b} \eta^{-1-2q} + C_a k^{\nu_b} \eta^{-q(1+3c_b^2)}. \quad (90)
\end{aligned}$$

For each mode, we have just written their k dependence, given by the constants $c_i(k)$, and their η dependence, discarding any numerical factor. As for the pre-bounce solution, we have used the factors C_a and X_a to include the case $\alpha = 0$. Let us explain how these factors arise. The coefficients C_a come because of the integration of $\tilde{\zeta}_b$ in Eq. (55). If α vanishes, this term is absent and the same modes come only through integration of Ψ_b , which contain, however, an extra $k^2 \eta^2$ factor. Finally, the X_a coefficients come from subtle cancellations in the solution for two perfect fluids $\alpha_a = 0$, which require some more discussion.

The first cancellation is in the integral of Ψ_b in Eq. (55). In fact, the integrand is an odd function of the background. In this situation, the pre-bounce, the Bounce and the post-bounce contributions cancel exactly, leaving no trace except for a decaying mode in the post-bounce. Successive recursions do not involve odd functions. The terms reappear multiplied by a k^2 , but with the same time dependence. This determines the X_a factors in Eqs. (87) and (88).

The second cancellation involves several integrals and can only be demonstrated using the exact solution of the two-fluid background (available in terms of hypergeometric functions). One has to pick out the integrals of Ψ in Ψ_b and $\tilde{\zeta}$ (the latter corrected by the contribution of Ψ_b to $\tilde{\zeta}$) and plug them into Eq. (57), where the cancellation occurs. This explains the X_a in Eqs. (89) and (90).

Comparing Eqs. (87)–(90) to Eqs. (67)–(70), we see that each mode in the pre-bounce gives rise to two modes in the post-bounce, one with the time-dependence of the homogeneous mode and one with the time dependence of the integral of the partner homogeneous mode. In some cases, these modes may be multiplied by $k^2 \eta^2$ or k^2 factors.

As in the simplified example of the previous section, also here Ψ has no constant mode with a possibly scale-invariant spectrum. At most, if there are no other modes dominating, the scale-invariant spectrum is carried by a decaying mode. This is hard to reconcile with experimental data. Nevertheless, we shall prove that there is always another dominant mode.

A. Discussion of the case $\alpha \neq 0$

All modes essentially depend on the characteristics of the background, which are encoded in the 3 parameters c_a^2 , Γ_a (or equivalently $q = 2/(1 + 3\Gamma_a)$), $c_b^2 = \Gamma_b$. However, c_a^2 comes always as a numerical coefficient and never enters the exponents of k and η . Following our policy of

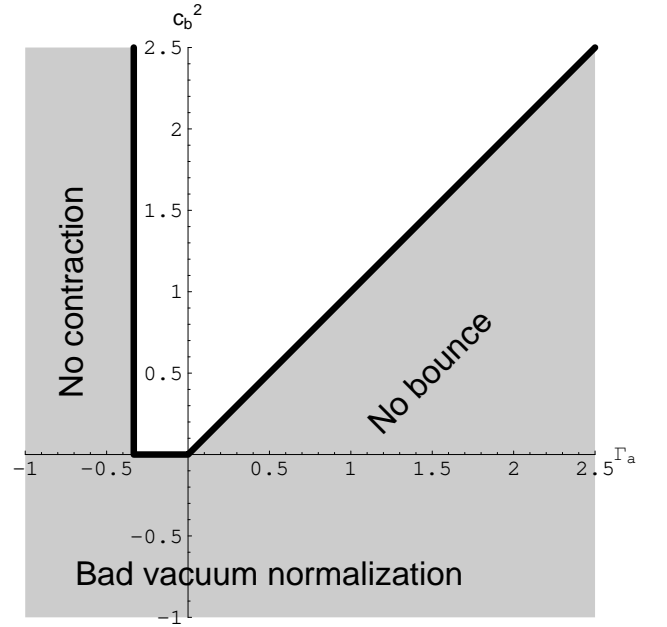


FIG. 3: In the plane (Γ_a, c_b^2) we show the interesting region for bouncing cosmologies in the case $\alpha \neq 0$. The shaded regions are excluded as giving no initial contraction, no bounce, or bad vacuum normalization of the secondary component.

discarding all numerical factors, we can discuss our results in terms of the remaining two parameters.

Of course, not all values of Γ_a and c_b^2 are relevant to bouncing cosmologies. In fact, in order to have a bounce, the ratio ρ_b/ρ_a must grow during contraction. This requires $c_b^2 > \Gamma_a$. Moreover, Γ_a should be greater than $-1/3$, in order to keep $q > 0$ and have an ordinary contraction. Finally, c_b^2 must be greater than zero for a correct vacuum normalization. The allowed region is shown in Fig. 3.

In principle, we should also exclude all values of $c_b^2 > 1$, since they cause fluctuations in the secondary component to propagate faster than light. However, since we are mainly interested in the effects of the kinematics of the bounce on the perturbations, in order to explore the slow evolution region $q < 1/2$, we shall also include the region $c_b^2 > 1$ in our analysis.

Comparing all the modes in Eqs. (87)–(90), we can distinguish four regions depending on the mode dominating each variable. These regions, shown in Fig. 4, and their

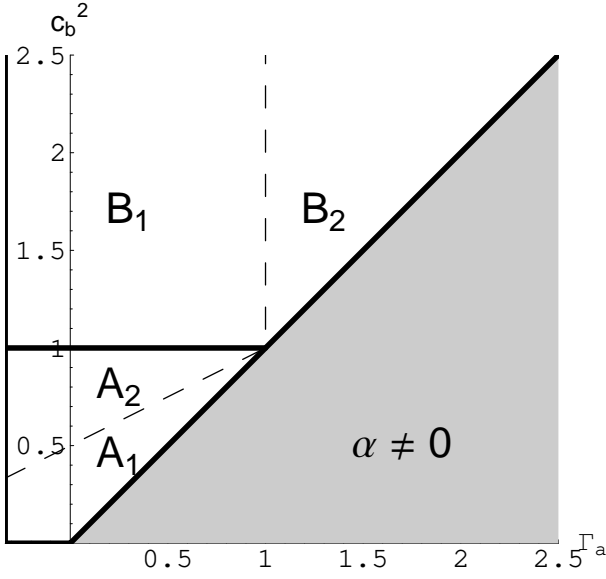


FIG. 4: In the case $\alpha \neq 0$, we have four regions. In regions A_1, A_2 the spectrum of the dominant component prevails in Ψ , while in regions B_1, B_2 , the spectrum of the secondary component prevails.

dominant modes are

$$A_1: \Psi \sim k^{\nu_a}, \tilde{\zeta} \sim k^{\nu_a} \eta^{-2},$$

$$\Psi_b \sim k^{\nu_a} \eta^{-1-q(1+3c_b^2)}, \tilde{\zeta}_b \sim k^{\nu_a} \eta^{-q(1+3c_b^2)} \quad (91)$$

$$A_2: \Psi \sim k^{\nu_a}, \tilde{\zeta} \sim k^{\nu_a} \eta^{-2},$$

$$\Psi_b \sim k^{\nu_a+2} \eta^{-2q}, \tilde{\zeta}_b \sim k^{\nu_a} \eta^{-1-2q} \quad (92)$$

$$B_1: \Psi \sim k^{-\nu_b}, \tilde{\zeta} \sim k^{-\nu_b} \eta^{-2},$$

$$\Psi_b \sim k^{-\nu_b+2} \eta^{-2q}, \tilde{\zeta}_b \sim k^{-\nu_b} \eta^{-1-2q} \quad (93)$$

$$B_2: \Psi \sim k^{-\nu_b} \eta^{1-2q}, \tilde{\zeta} \sim k^{-\nu_b} \eta^{-1-2q},$$

$$\Psi_b \sim k^{-\nu_b+2} \eta^{-2q}, \tilde{\zeta}_b \sim k^{-\nu_b} \eta^{-1-2q}. \quad (94)$$

The borders between the different regions are

$$A_1 - A_2: c_b^2 = \frac{1 + \Gamma_a}{2} \quad (95)$$

$$A_2 - B_1: c_b^2 = 1 \quad (96)$$

$$B_1 - B_2: \Gamma_a = 1. \quad (97)$$

We see that Ψ is dominated by the spectrum of the primary component for all bouncing cosmologies where the secondary component has $c_b^2 < 1$ (regions A_1 and A_2). Perturbations are also adiabatic, since $\zeta \sim \eta^2 \tilde{\zeta}$ is constant outside the horizon. On the contrary, for $c_b^2 > 1$, including also slowly evolving cosmologies ($\Gamma_a > 1$), Ψ is dominated by the spectrum of the secondary component. For $\Gamma_a > 1$ (region B_2), this mode is isocurvature, while for $\Gamma_a < 1$ (region B_1), this mode is adiabatic. The distinction between regions A_1 and A_2 comes from the different time dependence in Ψ_b and $\tilde{\zeta}_b$.

Allen & Wands studied a bounce where the principal component is a scalar field with a tracking potential, so

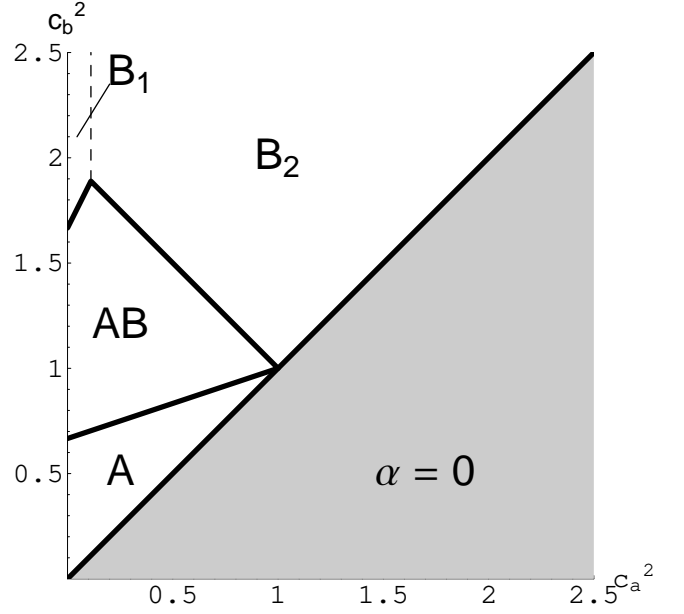


FIG. 5: In the case $\alpha = 0$, we have four regions. In regions A and AB the spectrum of the dominant component prevails in Ψ , while in regions B_1, B_2 , the spectrum of the secondary component prevails.

that $c_a^2 = 1$, but $\alpha_a \neq 0$ and Γ_a can assume any value between $-1/3$ and 0 . Their secondary component is a free ghost scalar field ($c_b^2 = 1, \alpha_b = 0$). Their case thus lies just on the border line between region A_2 and B_1 . From Eqs. (52) and (53), $\nu_a = \nu_b$ and the spectra of the two components coincide. They find that the final form of Ψ , after the homogeneous mode has decayed, is the one given in Eqs. (92) or (93).

B. Discussion of the case $\alpha = 0$

The case $\Gamma_a = c_a^2$ and $\Gamma_b = c_b^2$ contains all bounces developed by two perfect fluids or free scalar fields. In this case it is possible to write analytic solutions of the background in terms of hypergeometric functions, which are very useful to check for particular cancellations of modes, as explained before. In fact, all bounces described in this class enjoy time-reversal symmetry and thus the integrals of odd functions vanish. Therefore, the classification presented in the previous subsection has to be revised in order to take into account these cancellations. Furthermore, we cannot accept values $\Gamma_a = c_a^2 < 0$, for vacuum normalization reasons, and we are restricted to the upper half of the first quadrant.

Four different regions show up. They are illustrated in

Fig. 5 and are characterized by the following modes

$$A: \quad \Psi \sim k^{\nu_a}, \quad \tilde{\zeta} \sim k^{\nu_a} \eta^{-2}, \\ \Psi_b \sim k^{\nu_a} \eta^{-1-q(1+3c_b^2)}, \quad \tilde{\zeta}_b \sim k^{\nu_a} \eta^{-q(1+3c_b^2)} \quad (98)$$

$$AB: \quad \Psi \sim k^{\nu_a}, \quad \tilde{\zeta} \sim k^{\nu_a} \eta^{-2}, \\ \Psi_b \sim k^{-\nu_b+2} \eta^{-2q}, \quad \tilde{\zeta}_b \sim k^{-\nu_b} \eta^{-1-2q} \quad (99)$$

$$B_1: \quad \Psi \sim k^{-\nu_b+2}, \quad \tilde{\zeta} \sim k^{-\nu_b+2} \eta^{-2}, \\ \Psi_b \sim k^{-\nu_b+2} \eta^{-2q}, \quad \tilde{\zeta}_b \sim k^{-\nu_b} \eta^{-1-2q} \quad (100)$$

$$B_2: \quad \Psi \sim k^{-\nu_b+2} \eta^{3-2q}, \quad \tilde{\zeta} \sim k^{-\nu_b+2} \eta^{1-2q}, \\ \Psi_b \sim k^{-\nu_b+2} \eta^{-2q}, \quad \tilde{\zeta}_b \sim k^{-\nu_b} \eta^{-1-2q}. \quad (101)$$

The borders between the different regions are

$$A - AB: \quad c_b^2 = \frac{2 + c_a^2}{3} \quad (102)$$

$$AB - B_1: \quad c_b^2 = \frac{5}{3} + 2c_a^2 \quad (103)$$

$$AB - B_2: \quad c_b^2 = 2 - c_a^2 \quad (104)$$

$$B_1 - B_2: \quad c_a^2 = \frac{1}{9}. \quad (105)$$

The region where Ψ is dominated by the spectrum of the first component is enlarged towards $c_b^2 > 1$. This include regions A and AB . In regions B_1 and B_2 , Ψ gets the spectrum of the secondary component multiplied by k^2 . In B_1 , perturbations are adiabatic and in B_2 they are isocurvature. It is interesting to note how region B_1 has been reduced by the cancellation discussed above. Only in region A do $\tilde{\zeta}_b$ and Ψ_b take on the spectrum of the dominant component, while in all other regions they keep the original spectrum multiplied by k^2 . In region AB , therefore, we have coexistence of the two spectra in $\tilde{\zeta}_a$ and $\tilde{\zeta}_b$, though $\tilde{\zeta}$ is dominated by $\tilde{\zeta}_a$. This is an effect of the other cancellation discussed before.

VI. NUMERICAL SOLUTIONS

A numerical test of the above predictions has been performed by integrating the set of differential equations (43)–(46) using Mathematica. Initial conditions have been posed far from the bounce using the vacuum normalization prescription described in Sect. III D. The default Mathematica method for resolution of ordinary differential equations (which is a combination of Gear and Adams methods) cannot go through the bounce, because the step size falls to zero asymptotically as $\eta \rightarrow 0$. This is a consequence of the presence of \mathcal{H}^{-1} factors in the differential equations, which requires a high precision cancellation in the numerators. However, all variables and their derivatives have regular limits at the bounce, as can be explicitly checked on the so-obtained pre-bounce solutions. Thus a fixed step size method would overcome this problem. In fact, a standard Runge-Kutta method nicely follows the evolution of perturbations in any phases and in particular across the bounce. However, this method is

too slow to be employed for an extensive investigation of the parameter space. As a good compromise, we use the default Mathematica method far from the bounce, where it is faster than Runge-Kutta and as reliable. Only in the interval $|\eta| < 10^{-5}$ we switch to a Runge-Kutta method which allows us to cross the bounce. After the bounce we return to the default Mathematica method until horizon re-entry. The combination of the two methods then gives a very efficient and reliable numerical integrator for perturbations in bouncing cosmologies.

Since we are mainly interested in extracting the dominant mode at horizon re-entry, we have followed the evolution of two solutions with different k and we have evaluated the spectrum of the generic variable f in the set $\{\Psi, \tilde{\zeta}, \Psi_b, \tilde{\zeta}_b\}$ as

$$\frac{\log f_{k_1}(\eta_{re}) - \log f_{k_2}(\eta_{re})}{\log k_1 - \log k_2}, \quad (106)$$

where the subscripts 1 and 2 refer to the two solutions with different values of k , and η_{re} has been chosen of the order of $1/k$ but small enough to avoid contamination from the first oscillation. Of course, using more solutions would have given a more accurate and reliable fit of the spectrum, but it turns out that the accuracy of the simulation allows this simple and fast choice.

The other important prediction is on the time-dependence of the dominant mode, i.e. the exponent of η (hereafter we shall call it time index). This can be easily extracted as

$$\left. \frac{d \log f}{d \log \eta} \right|_{\eta=\eta_{re}}. \quad (107)$$

We have tested two cosmological models: a bounce with two perfect fluids, and a bounce with a scalar field endowed with a tracking potential plus a perfect fluid. In both cases the secondary fluid has negative energy density in order to trigger the bounce. We shall present the results separately.

A. Numerical testing of the two-perfect-fluid model

With this class of numerical simulations we can test the predictions of Sect. V B. We have spanned the plane (c_a^2, c_b^2) starting from $c_a^2 = 0.1$ up to $c_a^2 = 2$ with c_b^2 running from $c_a^2 + 0.1$ up to $c_b^2 = 2.5$, with steps of 0.1 in both parameters.

After the evaluation of the spectral and time index for all variables, just to have a global view of the parameter plane, we can draw contour plots for each index and compare these with the diagram of Fig. 5. These are shown in Fig. 6.

The orientation of the contours in the plots of Fig. 6a-d evidently shows the existence of two main regions of the parameter plane where the spectrum and the time dependence of the dominant mode in Ψ and $\tilde{\zeta}$ at re-entry are different. The calculated border line between

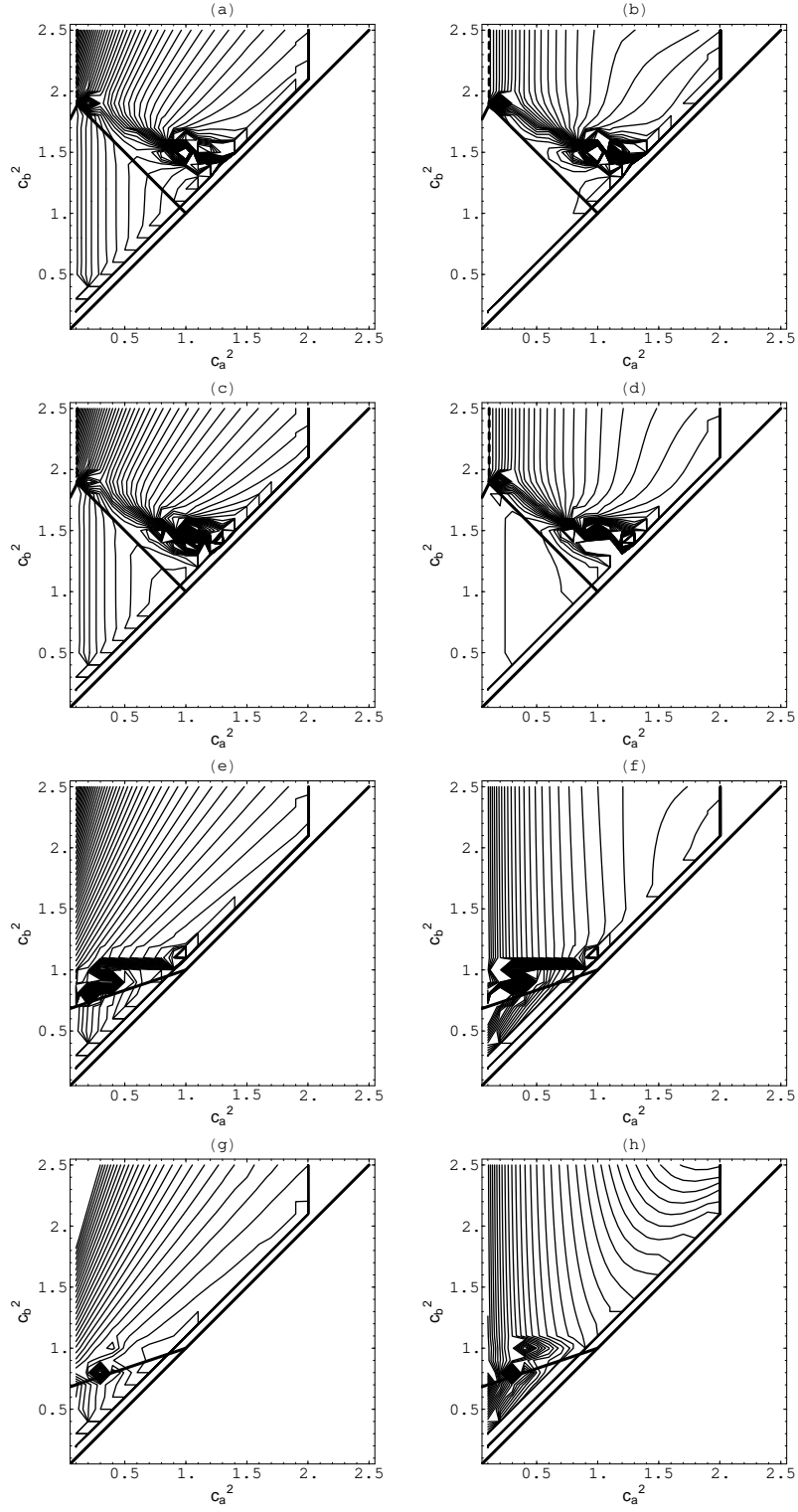


FIG. 6: On the left panels we have the contour plots of the spectral indices and on the right panels the time indices in the case $\alpha_a = \alpha_b = 0$. (a) and (b) refer to Ψ , (c) and (d) to ζ , (e) and (f) to Ψ_b , (g) and (h) to ζ_b .

region AB and region B_2 is superimposed in these figures. Actually, the numerical border line seems to be slightly higher towards larger values of c_b^2 . However, this border line is very sensitive to the choice of the evaluation time η_{re} . Taking different times we can see that the numerical border line tends to the theoretical one in the limit $\eta_{re} \sim 1/k$. In practice, one should keep in mind that close to the border line between regions AB and B_2 the two competing modes are comparable, giving rise to mixed initial conditions for the evolution inside the horizon. This also provokes glitches in the evaluation of the indices in these intermediate cases, which show up in our plots with a large density of contours on the upper side of the border line.

In Fig. 6e-h, the contours of spectral and time indices of Ψ_b and $\tilde{\zeta}_b$ are represented together with the border line of regions A and AB . With the same *caveat* as before, also this theoretical border line is respected.

Now, let us make a closer comparison between the theoretical values of the indices and those found numerically. In Fig. 7 we represent the results for a section of the plane (c_a^2, c_b^2) at fixed $c_a^2 = 0.1$ and varying c_b^2 . This line crosses three of the four theoretical regions, namely regions A , AB and B_1 . The numerical values are plotted along with the lines representing the theoretical behaviour of the indices. We can see that the agreement is very satisfactory for all gauge-invariant variables.

The spectra of Ψ and $\tilde{\zeta}$ are perfectly reproduced both in regions A , AB and in region B_1 , where they are dominated by the spectrum of the secondary fluid. The distinction between regions B_1 and B_2 is only in the time indices of Ψ and $\tilde{\zeta}$. In Figs. 7b,d we have also plotted as a dashed line the theoretical behaviour that these variables would have if region B_1 did not exist and there were only region B_2 . We see that while the numerical values change but are still compatible with the expectation of region B_1 , they cannot be compatible with the behaviour predicted by region B_2 .

The secondary fluid variables clearly show the transition between regions A and AB . Only one point in Ψ_c still seems to follow the dominant mode of region A rather than that of region AB for $c_b^2 = 0.7$. As already stated, this depends on a conservative choice of η_{re} , which eliminates contaminations from the oscillations but can sometimes select a not-yet-decayed mode in almost marginal cases like this.

The existence of several modes that are of the same order at η_{re} is particularly evident for $c_a^2 \sim 1$ and $c_b^2 \gtrsim 1$. In Fig. 8 we have plotted the numerical values for the time index of Ψ obtained for different choices of η_{re} , along the line in the parameter plane with $c_a^2 = 0.7$. A conservative choice such as $\eta_{re} = 0.4/(c_a k)$ leads to very good agreement with the theoretical values far from the border line, but the points with c_b^2 close to the border line between regions AB and B_2 tend to follow the behaviour of region AB . However, pushing η_{re} towards the first oscillation gives the necessary time to these points to feel the mode of region B_2 and align to the others. However,

the first oscillation globally alters all evaluations, which are displaced more and more from the theoretical super-horizon values. This discussion evidently shows that close to the border line the two competing modes contribute to determine the initial oscillations after horizon re-entry.

B. Numerical testing of the scalar-field model

In the second model of the bounce we have tested, the dominant fluid is replaced by a scalar field with an exponential potential. As shown in Ref. [15], the exponent of the potential determines Γ_a in the range $[0; 1]$. At the same time, c_a^2 is fixed to 1. With this model, we can thus test the theoretical predictions for the case $\alpha \neq 0$. However, the $\Gamma_a > 1$ part of the plane, which corresponds to region B_2 of Fig. 4, remains unexplored numerically. One more limitation arises at small c_b^2 , where viable bouncing backgrounds cannot be obtained. A complete study of this class of backgrounds has been done only in the case $c_b^2 = 1$ [15], so that the reasons why the dynamics does not flow in the same way for small c_b^2 remains unknown to us. However, since we are mainly interested in perturbations, we content ourselves with higher values of c_b^2 . This will be sufficient to distinguish regions A_1 , A_2 and B_1 , as we shall see.

It must also be said that in this case we have found it convenient to switch on a different set of differential equations close to the bounce. This set is the same as Eqs. (43)–(46) but with $a \leftrightarrow b$. In practice, to reduce numerical errors close to the bounce it is better to follow Ψ , $\tilde{\zeta}$, Ψ_a and $\tilde{\zeta}_a$. In this way, the whole numerical simulation is split in four phases: far pre-bounce, near pre-bounce, near post-bounce and far post-bounce.

Figure 9 is the analogue of Fig. 7 for the bouncing cosmologies where the dominant component is a scalar field. However, here, we have managed to find good backgrounds only starting from $c_b^2 = 0.5$. In all the spectra (Figs. 7a,c,e,g) the transition from region A_2 to region B_1 at $c_b^2 = 1$, as predicted in Sect. V A, is evident. Only one point testifies the existence of region A_1 , where we see that spectrum and time dependence of Ψ_b and $\tilde{\zeta}_b$ change.

VII. CONCLUSIONS

In this paper, we have addressed the problem of the evolution of perturbations in bouncing cosmologies by testing explicit regular models through the use of Einstein equations. At the moment, this is the only effective and conclusive way to carry out a theoretical investigation of the problem. In fact, in the absence of clean model-independent general arguments supporting any claim, the only answer can come from the study of regular bouncing models within the frame of General Relativity, where the evolution of perturbations can be followed explicitly from the initial state to the final horizon

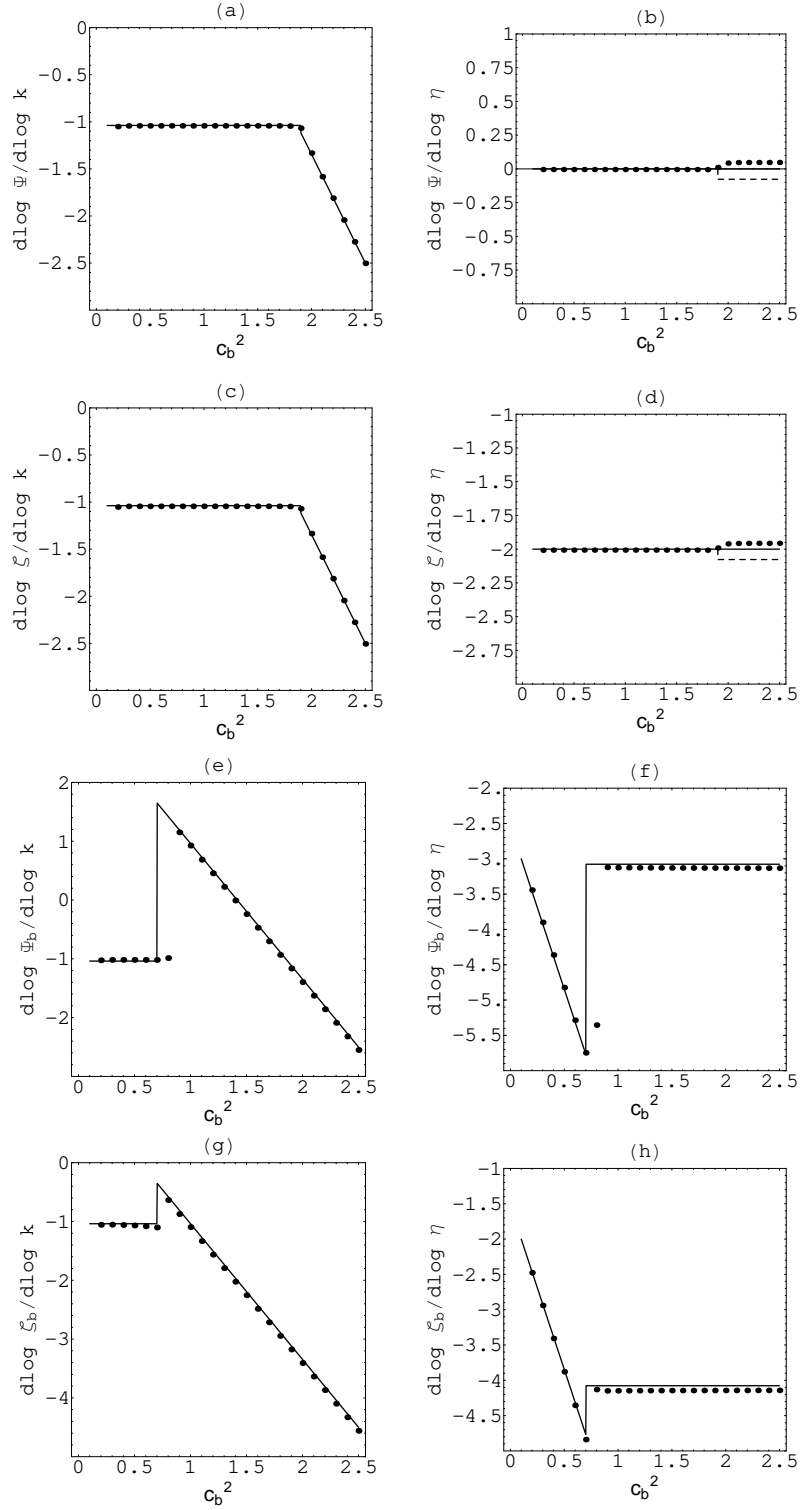


FIG. 7: On the left panels we have the spectral indices and on the right the time indices for our variables in the case $\alpha = 0$, keeping $c_a^2 = 0.1$ and varying c_b^2 . (a) and (b) refer to Ψ , (c) and (d) to ζ , (e) and (f) to Ψ_b , (g) and (h) to ζ_b .

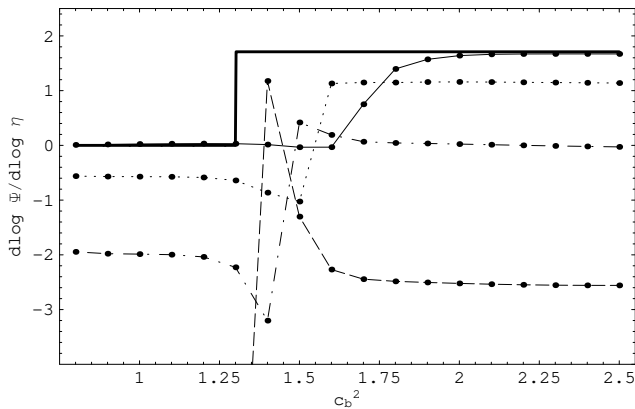


FIG. 8: Time index for Ψ for $c_a^2 = 0.7$ and varying c_b^2 . The evaluation has been done at different η_{re} . Points along the solid line are taken at $\eta_{re} = 0.4/(c_a k)$. The dotted line is obtained with $\eta_{re} = 1.5/(c_a k)$, the dot-dashed line with $\eta_{re} = 2.5/(c_a k)$, and the dashed line with $\eta_{re} = 3.5/(c_a k)$.

re-entry in the current expansion era.

Within classical general relativity, a bounce from contraction to expansion in spatially flat cosmologies can be realized only by violating the NEC. All high-energy corrections to General Relativity can thus be represented by a negative energy component in the Friedman equations, which is important only in the bounce phase. With this philosophy, we have completed a full study of a very wide class of bouncing cosmologies, with two non-interacting components, allowing the primary to have an intrinsic isocurvature mode, in order to describe scalar fields and perfect fluids at the same time. We have shown that the possibly scale-invariant spectrum of Ψ is carried by a homogeneous solution of the differential equations, which decays in the post-bounce phase. No other mode receives this spectrum, which is doomed to be only a transient characteristic of the Bardeen potential. If we use vacuum-normalized initial conditions for both components, we have explicitly shown that this decaying mode becomes subdominant w.r.t. some other mode before horizon re-entry. This general result appears to contradict some claims made in the literature, in particular those of Refs. [11] and [12].

As already explained in our previous paper [16], in Ref. [11], Eq. (26) provides an analytical solution $f(\eta) = \eta/(1 + \eta^2)^2$ for perturbations outside the horizon, which is valid both far from and through the bounce. However, the authors use an approximate form ($f_{app}(\eta) = 1/\eta^3$) of this solution far from the bounce and then match f_{app} to f just before the bounce. Had they used f from the beginning throughout the bounce, they would have found no mixing. No surprise, therefore, that the mixing they find is at order η^{-5} , which is just the next to leading order term in $f(\eta)$, which is missing in $f_{app}(\eta)$. Had they kept the η^{-5} term in $f_{app}(\eta)$ they would have found mixing at the order η^{-7} . We thus conclude that the mixing they find is just an artifact of their matching procedure. We also note that a recent paper [17] has criticized the

splitting of Ψ proposed by Ref. [11], into two separate variables Ψ_+ and Ψ_- which satisfy the same equation of motion as Ψ .

In the case of Ref. [12], the limit $\gamma \rightarrow 0$ ($k \rightarrow 0$ in our notation), used to evaluate the final spectrum, just selects the infrared modes at the bounce. However, the final spectrum should be evaluated at the horizon re-entry, after the decaying mode has gone away; it would correspond to $\gamma \rightarrow 0$ while keeping γz (our $k\eta$) of order 1.

The most important lesson from this class of models is probably contained in the simplified example of Sect. IV D. In fact, one may hypothesize any type of initial conditions for the perturbations of the secondary component, but one should then accept the basic facts, which are already included in the decoupled evolution of the perturbations of the dominant component. It should be concluded that in bouncing cosmologies with fast evolution ($q > 1/2$) the decaying mode of the Bardeen potential is always subdominant with respect to its constant mode, carrying a blue spectrum. In bouncing cosmologies with slow evolution ($q < 1/2$) the two modes are of the same order at horizon re-entry. But then, even in the case when no other isocurvature mode coming from coupling to other sources dominates, the late-time phenomenology would be different from the observed one [18].

There are at least three interesting directions in which this research may be extended.

The first is the study of more complicated models for perturbations, going beyond the relations (20)–(21). High-energy corrections may include higher derivatives and anisotropic stress, which are definitely outside the relations at the basis of our investigation. However, a first negative result already comes from Ref. [13], whose conclusions are similar to ours.

The second direction is in allowing an interaction or a correlation between the two components. A more realistic model, also closer to the original ekpyrotic proposal, should include the decay of the dominant component to radiation at the bounce. The implementation of such models with a coherent treatment of classical perturbation does not seem trivial.

Finally, the bounce integral may depend on an additional scale of the theory, which is independent of the curvature scale of the bounce. It is difficult to imagine a physical component with these characteristics. However, the possibility remains open.

In conclusion, all these possible extensions must invoke some special physics at the bounce in order to upset the basic result that the scale-invariant spectrum of the Bardeen potential is carried only by a decaying mode in the post-bounce. Up to now, no explicit construction of such a possibility has been presented in the literature and thus the claim that a scale-invariant spectrum can be carried by a constant Bardeen potential after a bounce remains an unproved conjecture.

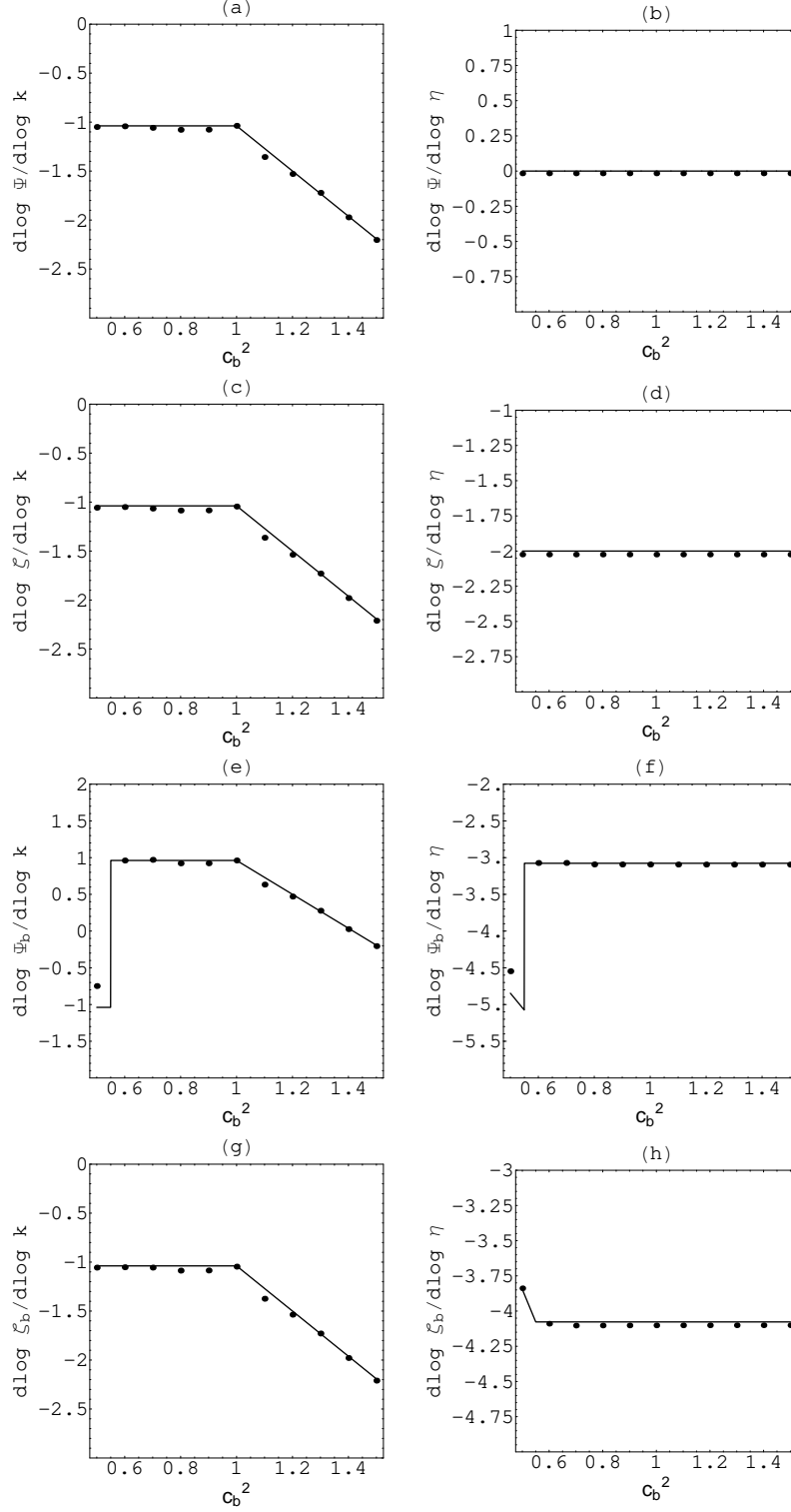


FIG. 9: On the left panels we have the spectral indices and on the right the time indices for our variables in the case $\alpha \neq 0$, keeping $c_a^2 = 0.1$ and varying c_b^2 . (a) and (b) refer to Ψ , (c) and (d) to ζ , (e) and (f) to Ψ_b , (g) and (h) to ζ_b .

-
- [1] G. Veneziano, Phys. Lett. B **265**, 287 (1991); M. Gasperini and G. Veneziano, Astropart. Phys. **1**, 317 (1993); R. Brustein, M. Gasperini, M. Giovannini, V. Mukhanov, and G. Veneziano, Phys. Rev. D **51**, 6744 (1995); M. Gasperini and G. Veneziano, Phys. Rep. **373**, 1 (2003).
- [2] J. Khoury, B.A. Ovrut, P.J. Steinhardt, and N. Turok, Phys. Rev. D **64**, 123522 (2001) and Phys. Rev. D **66**, 046005 (2002); S. Gratton, J. Khoury, P. J. Steinhardt, and N. Turok, Phys. Rev. D **69**, 103505 (2004); A. J. Tolley, N. Turok, and P. J. Steinhardt, Phys. Rev. D **69**, 106005 (2004).
- [3] P. Horava and E. Witten, Nucl. Phys. B **460**, 506 (1996) and B **475**, 94 (1996).
- [4] V.F. Mukhanov, H.A. Feldman, and R.H. Brandenberger, Phys. Rep. **215**, 203 (1992).
- [5] K. Enqvist and M. S. Sloth, Nucl. Phys. B **626**, 395 (2002); D. H. Lyth and D. Wands, Phys. Lett. B **524**, 5 (2002).
- [6] V. Bozza, M. Gasperini, M. Giovannini, and G. Veneziano, Phys. Lett. B **543**, 14 (2002); Phys. Rev. D **67**, 063514 (2003).
- [7] D. Lyth, Phys. Lett. B **524**, 1 (2002); R. Brandenberger and F. Finelli, JHEP **0111**, 056 (2001); D. Lyth, Phys. Lett. B **526**, 173 (2002); J. Hwang, Phys. Rev. D **65**, 063514 (2002); S. Tsujikawa, Phys. Lett. B **526**, 179 (2002); J. Martin, P. Peter, N. Pinto-Neto, and D.J. Schwarz, Phys. Rev. D **65**, 123513 (2002); J. Hwang and H. Noh, Phys. Lett. B **545**, 207 (2002); J. Martin, P. Peter, N. Pinto-Neto, and D. J. Schwarz, Phys. Rev. D **67**, 028301 (2003); S. Tsujikawa, R. Brandenberger, and F. Finelli, Phys. Rev. D **66**, 083513 (2002); C. Cartier, R. Durrer, and E. Copeland, Phys. Rev. D **67**, 103517 (2003); P. Peter, N. Pinto-Neto, and D. A. Gonzalez, JCAP **0312**, 003 (2003); P. Creminelli, A. Nicolis, and M. Zaldarriaga, Phys. Rev. D **71**, 063505 (2005).
- [8] N. Deruelle and V.F. Mukhanov, Phys. Rev. D **52**, 5549 (1995).
- [9] R. Durrer and F. Vernizzi, Phys. Rev. D **66**, 083503 (2002).
- [10] J. Hwang and H. Noh, Phys. Rev. D **65**, 124010 (2002); C. Gordon and N. Turok, Phys. Rev. D **67**, 123508 (2003); J. Martin and P. Peter, Phys. Rev. D **68**, 103517 (2003); J. Martin and P. Peter, Phys. Rev. Lett. **92**, 061301 (2004); N. Deruelle and A. Streich, Phys. Rev. D **70**, 103504 (2004); J. Martin and P. Peter, gr-qc/0406062.
- [11] P. Peter and N. Pinto-Neto, Phys. Rev. D **66**, 063509 (2002).
- [12] F. Finelli, JCAP **0310**, 011 (2003).
- [13] C. Cartier, hep-th/0401036.
- [14] M. Gasperini, M. Giovannini and G. Veneziano, Phys. Lett. B **569**, 113 (2003); Nucl. Phys. B **694**, 206 (2004).
- [15] L. Allen and D. Wands, Phys. Rev. D **70**, 063515 (2004).
- [16] V. Bozza and G. Veneziano, hep-th/0502047.
- [17] G. Geshnizjani and T. J. Battefeld, hep-th/0506139.
- [18] L. Amendola and F. Finelli, astro-ph/0411273.